Full Length Article

On-purpose production of propane fuel gas from the hydrothermal reactions of n-butanol over Pt/Al$_2$O$_3$ catalyst: A parametric and mechanistic study

Onajite T. Abafe Diejomaoh [a], Jude A. Onwudili [a,c,*], Keith E. Simons [b], Priscila Maziero [d]

[a] Energy and Bioproducts Research Institute, College of Engineering and Physical Sciences, Aston University, Birmingham B4 7ET, UK
[b] Sustainable Fuels, SHV Energy, 2132 JL Hoofddorp, the Netherlands
[c] Department of Chemical Engineering and Applied Chemistry, College of Engineering and Physical Sciences, Aston University, Birmingham B4 7ET, UK
[d] Biofuels Development Manager, Supergasbras, Av. Santa Catarina, 2461 - Vila Mascote, São Paulo - SP 04378-500, Brazil

ARTICLE INFO

ABSTRACT

Production of components of liquefied petroleum gases (LPG) from biomass can become a sustainable pathway towards the defossilisation of off-grid locations for heating and transport applications. The reactions of butanol in the presence of 5 wt% Pt/Al$_2$O$_3$ across a set of reaction temperatures (200 °C to 300 °C), reaction times (up to 2 h), n-butanol concentrations (up to 30 wt%) and various feedstock-to-catalyst mass ratios were investigated and optimised. High conversion of n-butanol to gas products (99.91 wt%), high yield of propane (63.56 wt%) and propane hydrocarbon selectivity of 88.87 % were achieved in a batch reactor after 2 h of reaction at 300 °C. The formation of propane appeared to be from several mechanisms including decarbonylation, dehydration, C–O and C–C hydrogenolysis and hydrogenation. Significant yields of hydrogen and butane were formed, which may support the complex mechanistic pathways involved in n-butanol conversion. The 5 wt% Pt/Al$_2$O$_3$ catalyst was stable for up to two reaction cycles under the conditions investigated before mainly deactivating via hydrolysis of the alumina support and coke formation. This present work shows that n-butanol is a potential bio-derived feedstock to produce on-purpose biopropane fuel gas via catalytic hydrothermal processing.

1. Introduction

Fossil-LPG (liquefied petroleum gases) component gases such as propane and butane with a global demand in excess of 300 million tonnes per year. These gases are recognised as major fuels characterised by higher energy efficiency and lower carbon intensity than any other fossil-based fuels used in transportation and heating [1]. However, as with other fossil-based fuels, they are non-renewable and contribute to global CO$_2$ emissions when combusted. To minimise the impact of impending global environmental and energy crisis, the UK has made ambitious commitment to implement ways to decarbonize the energy sector through clean and sustainable alternative fuels [2].

Biomass is a sustainable resource of energy [3,4] as utilisation of bio-derived fuels can be regarded as CO$_2$ neutral [5,6]. For this reason, bio-derived LPG (Bio-LPG) obtained from biomass with chemical similarity to fossil-LPG has been recently introduced. Bio-LPG is seen as a reliable

fuel for off-grid areas [7] with potentials to make significant contribution towards the attainment of Net Zero carbon emission. For instance, Bio-LPG has been reported to reduce GHG emissions by up to 78 % [8]. In addition, the combustion of Bio-LPG releases 27 % less nitrogen oxides (NOx) and 43 % less particulate matter compared with oil [7], leading to improved air quality. The growing annual demand for LPG, similar to that of aviation fuel (371 billion litres pre-Covid), highlights the timeliness for efficient and sustainable routes for the production of bio-LPG. The United Kingdom (UK) has seen the demand for bio-propane increase by 39 % since the year 2000 [7,9]. Current industrial setups for the large-scale production of bio-LPG are only capable of approximately 5——8 % yield of bio-propane as by-products of the hydro-processing of vegetable fats and oils (HVO process) [7,10]. Current understanding is that the efficient utilisation of existing and upcoming HVO plants around the world, could lead to an estimated production volume of approximately 294,000 tonnes of bio-propane

[7,10].

Recent studies have reported the catalytic processing of various biomass-derived feedstocks such as C_4-C_5 carboxylic acids [11–13] and alcohols [12,14,15] over transition metal catalysts as a green route to produce bio-propane or bio-butane. For instance, Mazziota et al. 2017 [14] achieved dehydrogenation and decarbonylation of a series of primary alcohols to hydrocarbons with one carbon unit less over ruthenium-based catalyst. The production of propane as by-product from aqueous-phase reforming of n-butanol over Ni/Al_2O_3 and Ni/CeO_2 catalysts have also been noted [12]. In addition, Jasper and Dirk [13] converted citric acid to methylsuccinic acid over Pd/C and Pt/C as catalyst and obtained propane amongst other products by dehydration, decarboxylation and hydrogenation in the presence of hydrogen. In their study, Jiang et al. [16], efficiently obtained bio-butane from levulinic acid over platinum on carbon support as catalyst. Previous work showed that butyric acid could be converted to propane using 5 wt% platinum catalyst on carbon support via a decarboxylation reaction [11]. Recently, a series of single and mixtures of transition metal catalysts including Pt/C have been investigated for the conversion of glycerol (obtained as by-product of bio-diesel production from triglyceride) to gaseous products such as propane [15].

The choice of bio-derived feedstock for Bio-LPG production is important for overall process viability, especially if they can be obtained from lignocellulosic biomass resources [17]. In most cases, C_4 oxygenates such as butyric acid, hydroxybutyric acid and butanol have been identified as potential bio-derived feedstocks for bio-propane production [9]. Previous on-purpose bio-propane production [9,10] showed that butyric acid was a promising feedstock as butyric acid can be obtained as an intermediate product from the well-known acetone-butanol-ethanol (ABE) fermentation process but obtaining it in large quantities would mean disrupting the entire fermentation process, which may be technically challenging. Alternatively, n-butanol, which is one of the main final products of ABE fermentation may be a better feedstock. N-butanol accounts for 60 % and 71 % of products, respectively, in traditional batch and continuous ABE fermentation processes [17]. In addition, n-butanol has a low vapour pressure, low toxicity, low flammability as well as a milder smell (sweet, banana-like) than butyric acid (rancid butter).

Giving that biological processing of biomass to low molecular weight oxygenates occur in aqueous medium, it will be important to find appropriate conversion methods of these compounds to desired products without isolation or extensive purification. This would save on substantial energy costs and enhance the viability of the process route, making the final products more affordable. Therefore, the main aim of this work was to understand the catalysed reactions of aqueous solutions of n-butanol for on-purpose production of propane at high yields and high selectivity under hydrothermal conditions The investigation of the effects of reaction parameters on n-butanol conversion and product yields were carried out in a batch reactor. The parameters studied included reaction temperatures (200 °C − 300 °C), reaction times (up to 2 h), n-butanol concentrations (10 wt% − 30 wt%) and various feedstock-to-catalyst mass ratios. The experimental results were used to gain insight into the prevailing reaction mechanisms that lead to the final products, with the objectives of optimising the conversion process to maximise propane production. The stability of the catalyst under the conditions used in this present study was examined as an indication of its long-term viability.

2. Materials and methods

2.1. Materials

n-Butanol (99 % purity) was purchased from Acros Organics (CAS 71 36–3) and used as received. Platinum on alumina support (5 wt% Pt/Al_2O_3) catalyst was obtained from Catal International Limited, Sheffield, United Kingdom and was used as received. The characteristics of the catalysts have been reported in an earlier publication but briefly; the bulk density was 720 kg m^{-3}, BET surface area of 182 m^2 g^{-1}, pore diameter of 9.00 nm, average particle size of 30 μm, pore volume of 0.7 cm^3 g^{-1} and actual Pt metal content of 5.07 wt% [18]. Deionised water was obtained from a Milli-Q Advantage A10 Water Purification System.

2.2. Experimental and analytical methods

The experimental procedure used for this work is schematically presented in Scheme 1.

2.2.1. Hydrothermal processing of n-butanol

The hydrothermal reaction for the decarbonylation of butanol was performed in a Hastelloy-C batch reactor with 100 mL capacity purchased from Parr Instruments Co., Inc., Moline, IL, USA. The experimental procedure was modified from a previous work by our research group [19]. The reactor was loaded with the various amount of butanol (2 g to 6 g) in deionised water to make a 20 mL feedstock solution and 5 wt% Pt/Al_2O_3 (catalyst added. Thereafter, the reactor was sealed, purged and pressurised with 5 bars of nitrogen used as internal standard for the quantification of the gaseous products by gas chromatography. The reactor was then heated to the desired temperature for a set time (Table 1) by placing it into an electric heating jacket equipped with a temperature controller. At the end of each experiment, the reaction was stopped by removing the reactor from the heating jacket and allowed to cool rapidly to below 30 °C with the aid of an industrial cooling fan. The experimental parameters studied are shown in Table 1.

After cooling, the temperature and pressure were recorded, and the gas products were collected into a 1 L Tedlar bag and immediately analysed with GC-FID/TCD. The reactor was then emptied, and the catalyst separated out of the aqueous phase by vacuum filtration. The catalyst was dried to a constant weight in an oven at 105 °C for 2 h while the liquid products was analysed with GC–MS to identify and quantify any unreacted n-butanol and any intermediate or formed organic compounds. To establish reproducibility, triplicates of selected experiments were performed and analysed. The obtained results were reproducible with standard deviation less than ± 5 % for conversion of n- butanol or yield of propane.

2.2.2. Analysis of gas products

The analysis of gas products in this study followed an in-house validated procedure. The products were analysed by manually injecting 0.6 μL of the gas sample into a Shimadzu GC-2014 gas chromatograph equipped with a thermal conductivity detector (for carbon dioxide and permanent gases) and gas chromatography with flame ionisation detector (for hydrocarbons) [19,20]. The injection port temperature was set at 80 °C. Separation of carbon dioxide and permanent gases such as hydrogen, nitrogen, oxygen, and carbon monoxide was effected on a 5 Å, 60/80 mesh, 2 m × 2 mm ID molecular sieve column; while the separation of hydrocarbons was effected on a Hayesep 80–100 mesh, 2 m × 2 mm column. The column oven temperature was initially held at 80 °C and ramped at 10 °C min^{-1} to 180° C and then held at 180 °C for 3 min, with a total analysis time of 13 min. The detector (FID) temperature set at 220 °C.

The volume percent of each gas produced were calculated from their peak area and was used to determine the masses of gases produced according to the ideal gas Equation (1).

$$Mass\ of\ gas\ component\ m_i = \frac{P_i \times V \times M_i}{RT} \quad (1)$$

where m_i is mass of gas (g), P_i is partial fraction of each component (Pa), V is volume of gas (reactor headspace in m^3 × volume fraction of gas m_i), M_i is relative molecular mass (g/mol), R is gas constant (8.314 J mol^{-1}K^{-1}) and T is the temperature of the reactor after cooling (K). The amount of dissolved CO_2 in the aqueous phase was calculated from
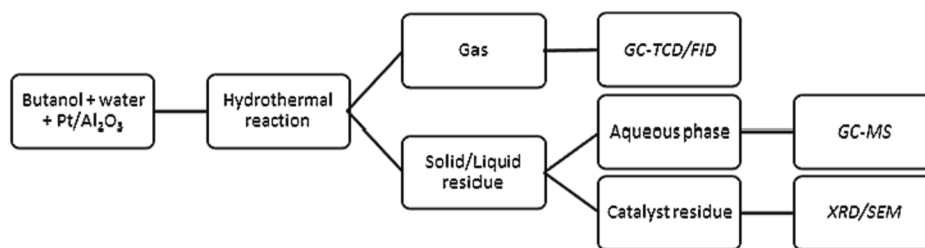
Scheme 1. General experimental and analytical procedure for gases, liquid and solids.

Table 1
Experimental programme used in this present work.

Feedstock loading (n-butanol) (g)	5 wt% Pt/Al$_2$O$_3$ (g)	Reaction temperature (°C)	Residence time (h)
2	No catalyst	200	0.5
3	0.01	250	1.0
4	0.25	300	2.0
6	0.50		

Henry's Law [19].

Based on the result obtained, the actual gas yield (%) for the gases were calculated from Equation (2).

$$Yield\,of\,gas\,componenti(\%) = \frac{m_i}{m_{butanol}} \times 100 \quad (2)$$

Hydrocarbon selectivity towards the gas products was calculated based on Equation (3).

$$Hydrocarbon\,selectivity(\%) = \frac{Yield\,of\,hydrocarbon\,gas\,component}{\sum Yields\,of\,all\,hydrocarbon\,gases} \times 100 \quad (3)$$

The conversion of carbon atoms in the n-butanol feed to carbon-containing gas products was calculated as carbon gasification efficiency (CGE) using Equation (4).

$$CGE, (\%) = \frac{\sum Mass\,of\,carbon\,atoms\,in\,gas\,products}{Mass\,of\,carbon\,atoms\,in\,n-butanol\,feed} \times 100 \quad (4)$$

2.3. Analysis of liquid products

The liquid product was extracted using ethyl acetate and analysed using a Shimadzu Gas chromatograph GC-2010 Plus coupled to Shimadzu Single Quadrupole Mass Spectrometer (QP2010 SE) equipment [18]. The column used was a DB-5 ms capillary column with an inner diameter of 0.25 mm and length of 30 m. Helium was used as the carrier gas at a constant flow rate of 1.5 mL min^{-1}. A sample volume of 1 μL was injected into the GC column via an injection port maintained at 280 °C, with 50.0 split ratio. The GC oven was initially held at 50 °C for 5 mins, then ramped at 10 °C min^{-1} to 280 °C, and finally held at 280 °C for 2 min, giving a 31 mins analysis time. Compounds separated on the column were detected by the mass selective (MS) detector held at 250 °C. The transfer line was also kept at a temperature of 275 °C. Mass spectra were obtained using 70 eV ionization energy in the molecular mass range of $m/z = 35$–300, with a scan time of 0.35 s. The peaks were identified with the aid of a National Institute of Standards and Technology (NIST, 2020 Version) library installed on the MS. Quantitative analysis of n-butanol was carried out by external standard method. N-butanol conversion was calculated based on Equation (5).

$$Conversion(wt\%) = \frac{mass\,of\,butanol\,feed\,-\,mass\,of\,unreacted\,butanol}{mass\,of\,butanol\,feed} \times 100 \quad (5)$$

2.4. Catalyst stability test

Prior to the catalyst stability test, specified amount of the 5 wt% Pt/Al$_2$O$_3$ catalyst was calcined in a muffle furnace under nitrogen flow. The operating temperature was set to 550 °C with a ramp rate of 5 °C min^{-1} and held for 2 h at the set temperature. The total heating time per run was 3 h, 45 mins.

The spent 5 wt% Pt/Al$_2$O$_3$ was recovered after each experiment by vacuum filtration and dried at 60 °C for 24 h in an oven. Thereafter, the required amount of catalyst was either first calcined or directly used in the reaction system for the second cycle under the same reaction conditions. The same catalyst was used during three cycles under the same condition.

2.5. Catalyst characterization

2.5.1. Xray diffraction analysis

Fresh and recovered catalyst were analysed with X-ray Diffraction (XRD), performed on a Bruker D8 Advance diffractometer. The analysis was performed with Cu Kα1,2 radiation (40 mA and 40 kV, 0.02 mm Ni Kβ filter and 2.5° Soller slits, with a scan from 5 to 105°). The fresh and recovered catalysts were loaded on top of PMMA specimen holders and the diffractograms were collected in the Bragg–Brentano geometry with a step scan of 0.02° (1 s per step). Peaks on the diffractograms were assigned based on the International Centre for Diffraction Data's (ICDD) Powder Diffraction File-2 2012 (PDF-2 2012) and Inorganic Crystal Structure data bases ICSD.

2.5.2. Scanning electron microscopy (SEM) analysis

Scanning electron microscopy (SEM) images before and after reactions were taken for the catalysts using a JEOL JSM-7800F Prime high-resolution scanning electron microscope with 8 – 10 kV acceleration. The samples were held on carbon tape on the holder and analysed.

3. Results and discussion

3.1. Effect of reaction temperature on n-butanol conversion and gas yields

The effect of temperature on the conversion of butanol to bio-LPG was investigated by reacting 10 wt% of butanol in water with 0.25 g of 5 wt% Pt/Al$_2$O$_3$ as catalyst at 200 °C, 250 °C and 300 °C for 1 h each. The molar ratio of n-butanol in the feedstock to Pt metal in the catalyst used for this work was 421. The temperature range was chosen based on our previous parametric study on biopropane production from butyric acid and to maximize the conversion of the feedstock while ensuring a temperature as mild as possible as reports show that thermal decomposition of butanol becomes negligible at higher temperature. The results obtained with respect to gas yield, propane selectivity and conversion of butanol are presented in Fig. 1. It was observed that an increase in the reaction temperature from 200 °C to 300 °C resulted in overall increase of the yields of gaseous products and conversion of butanol. The results showed that propane was the dominant gas component followed by CO$_2$ across all the conditions tested in relation to reaction temperature. The yield of propane was found to increase by a
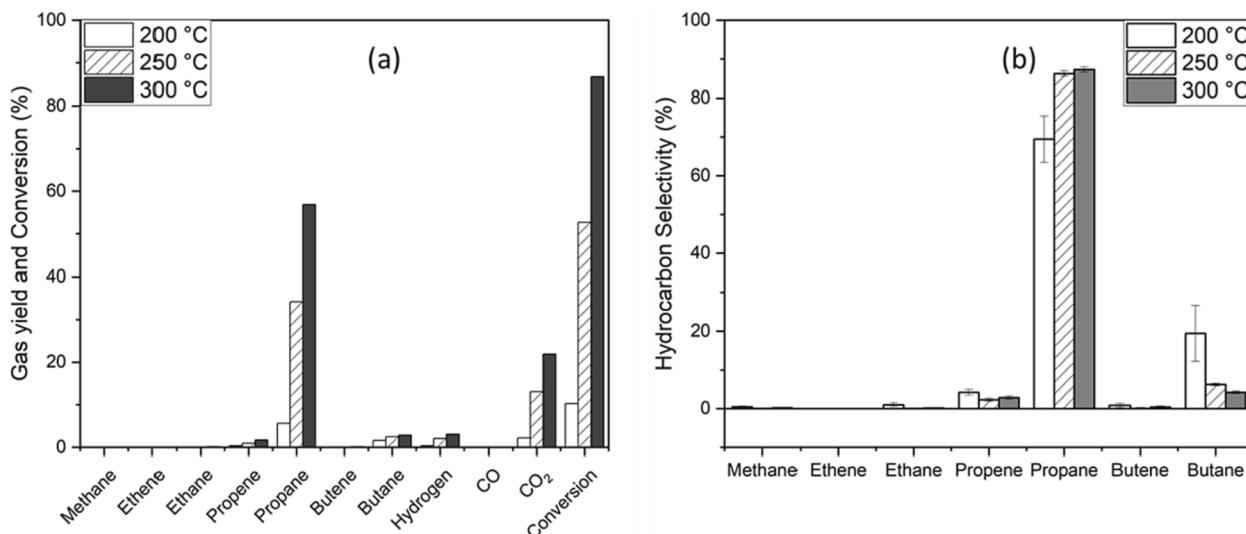
Fig. 1. Effect of reaction temperature on: (a) the yield of gases and conversion of 10 wt% aqueous n-butanol; (b) selectivity of hydrocarbon gases, using 0.25 g 5 wt% Pt/Al$_2$O$_3$ catalyst (Reaction conditions: n-butanol/Pt metal molar ratio = 421:1); initial pressure of N$_2$, 5 bar; autogenic pressure of 7.7 bar, 18.7 bar and 26.6 bar at 200 °C, 250 °C and 300 °C, respectively).

factor of 10 from 5.61 % at 200 °C to 56.88 % at 300 °C. Interestingly, the yields of hydrogen and CO$_2$ also increased by approximately 10 times (Fig. 1a), indicating the link among the reactions leading to the formation of these three gases. Furthermore, the yield of other prominent gases such as hydrogen, propene, butene and butane also increased with temperature, suggesting increased n-butanol conversion with the occurrence of other favourable reactions.

Using equation (5), the hydrocarbon selectivity was calculated in relation to temperature and presented in Fig. 1b. The results showed that propane was the dominant hydrocarbon gas component across all three temperatures, with a selectivity of 92.1 % at 300 °C. Moreover, the results from Fig. 1a and Fig. 1b showed some interesting trends in the yields and selectivity of propene, butane and hydrogen. While the yields of these three gases remained much lower than those of propane, Fig. 1a shows that they increased with increasing temperature from 200 °C to 300 °C. However, Fig. 1b shows that the selectivity towards propene and butane decreased in favour of that of propane with increasing temperature. These observations may indicate the trends in the most dominant reaction mechanisms in relation to increasing temperatures (See Section 3.5), with a number of possible pathways leading to propane in the presence of the selective Pt/Al$_2$O$_3$ catalyst [21,22].

3.2. Effect of reaction time on n-butanol conversion and yields of gas products

From Section 3.1, it became clear that the reaction at 300 °C produced the highest yield of propane from n-butanol. Hence, the effect of reaction time on n-butanol conversion was carried out with 0.25 g of 5 wt% Pt/Al$_2$O$_3$ for reaction times from 0 h to 2.0 h. The concentration of n-butanol was fixed at 10 wt%. The time of "0 h" referred to experiments that were stopped once the set temperature was reached. The result obtained are presented in Fig. 2, which shows that propane was the dominant component in the gas product in all cases and consistently increased with increasing reaction times and with corresponding increases in n-butanol conversion. However, hydrogen and butane were formed, and their yield increased slightly with increasing reaction times. Their continued presence in the gas product indicated that the mechanisms of their formation remained active throughout the experiment. Butanol deoxygenation mechanism of dehydration to butene followed by hydrogenation to butane as well as C-O hydrogenolysis of n-butanol directly to butane have been reported [21,23].

Fig. 2 shows a rapid production of gases within the first 0.5 h followed by a slower increase with longer reaction times. The yield of the gases produced after 1 h were in the order; butane (2.86 %) < hydrogen
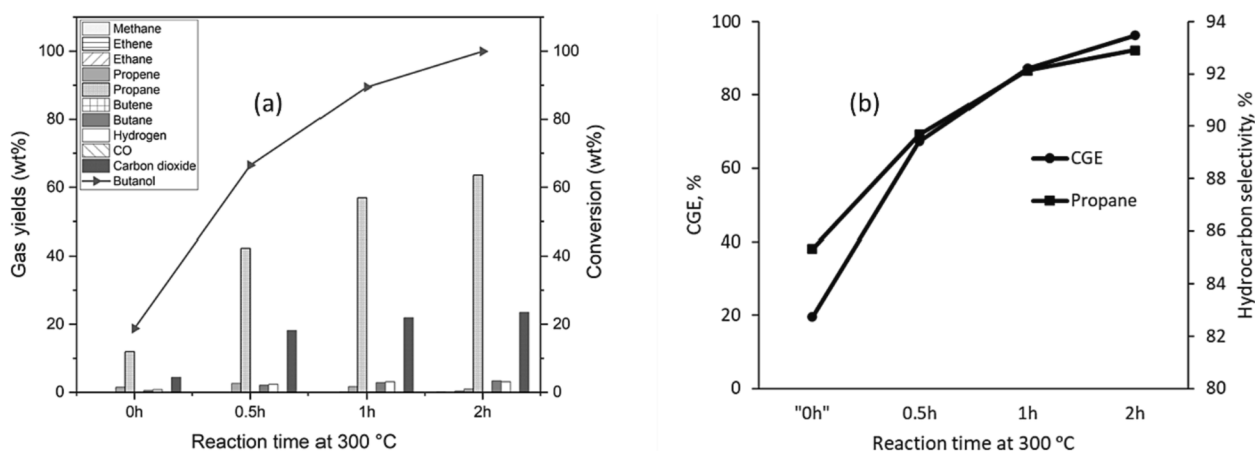

Fig. 2. Effect of reaction time on the conversion of 10 wt% aqueous n-butanol to gas products at 300 °C (Reaction conditions: 0.25 g of 5 wt% Pt/Al$_2$O$_3$ (n-butanol/Pt metal molar ratio = 421:1); initial pressure of N$_2$ of 5 bar).

(3.08 %) < carbon dioxide (21.91 %) < propane (56.88 %). Extending the reaction time from 1 h to 2 h resulted in continuous but much slower increase in gas formation due to the reduced concentration of n-butanol after the initial rapid conversion. Hence, after 1 h of reaction, butanol conversion was approximately 86.74 % and increased to 99.91 % after 2 h. Correspondingly, propane yield increased from approximately 56.88 % after 1 h to 63.56 % after 2 h, amounting to an 11.7 % increase. During this time, the yield of carbon dioxide increased from 21.91 % to 23.47 %, which was a smaller increase of 7.12 % compared to the yield of propane. For the other gases, little or no change in their yields were observed. These changes in the conversions of butanol and the yields of propane and CO_2, may support the hypothesis that propane formation occurred via more than one reaction pathways [21,22] as discussed in Section 3.4.

3.3. Effect of catalyst loading

The effect of catalyst loading on the hydrocarbon selectivity, product yield and butanol conversions was determined by performing experiments without the use of catalyst and with catalyst loading (5 wt% Pt/ Al_2O_3) of 0.1 g, 0.25 g and 0.5 g corresponding to n-butanol/Pt metal molar ratios of 1053:1, 421:1 and 211:1). The reactions were carried out at 300 °C and residence time of 1 h. The results obtained are presented in Fig. 3a. The results obtained for the experiment without the use of Pt/ Al_2O_3 showed that the reaction hardly took place, with only 1.47 % of butanol converted and a propane yield was 0.47 wt%.

On the other hand, the experiments with Pt/Al_2O_3 led to a dramatic increase in both n-butanol conversion and propane yields. The results obtained for butanol conversion and propane yield were found to be 43.32 % and 23.97 % with 0.10 g loading of 5 wt% Pt/Al_2O_3, 89.41 % and 56.88 % with 0.25 g of Pt/Al_2O_3 and 99.8 % and 55.04 % with 0.50 g of Pt/Al_2O_3, respectively. The results showed an 11.6 % increase when the catalyst loading increased from 0.25 g to 0.5 g, leading to almost complete conversion. Interestingly, the propane yield was found to decrease slightly at the highest catalyst loading, which indicated to the promotion of other side reactions. For example, the formation of butane doubled when catalyst loading was doubled from 0.25 g to 0.5 g. In their modelling and experimental studies, Gürbüz et al. [23] found that butanol conversion under non-aqueous environments proceeded via C-O hydrogenolysis to form butane or decarbonylation of butanol/butanal to propane. While under different reaction atmospheres/medium, some similarities and differences in reaction pathways would exist between butanol conversion in non-aqueous and the hydrothermal media used in this present work. Hence, giving that the yield of propane remained significantly (>20 times) higher than those of butane, decarbonylation appeared to be the dominant mechanism over C-O hydrogenolysis at all

catalyst loadings used in this work. However, increasing the catalyst loading to 0.5 g provided more active sites for C-O hydrogenolysis, leading to the doubling or butane yield. Fig. 3a shows that, nearly equal yields of propene (0.43 wt%) and propane (0.47 wt%) were obtained during the non-catalytic test, when n-butanol conversion was only 1.47 %. This indicated that the hydrothermal conversion of n-butanol required catalysis and that without catalysts the small amount of butanol converted was non-selective towards propane. However, the use and increased loading of catalyst effectively increased n-butanol conversion, the suppression of propene formation and a corresponding high selectivity towards propane formation (Fig. 3b). Indeed, propane selectivity increased in parallel with n-butanol conversion in Fig. 3a and hydrocarbon selectivity in Fig. 3b. Even though n-butanol conversion increased when 0.5 g of the catalyst was used, propane selectivity decreased slightly to 85.5 %, corresponding to slight increase in butane yield. This indicated possible stronger Pt-carbon bonding, leading to char formation or enhanced C-O hydrogenolysis to produce butane [23]. Thus, 0.25 g of 5 wt% Pt/Al_2O_3 was found as the optimal loading of the catalyst for the conversion of n-butanol to produce propane with minimal side reactions.

3.4. Effect of n-butanol concentration

Based on temperature and catalytic investigations, it was found that 0.25 g of 5 wt% Pt/Al_2O_3 could convert 10 wt% butanol to give the target propane gas in high yields up to 56.88 % at 300 °C after 1 h of reaction. Converting high concentrations of feedstocks and achieving high selectivity of desired products would be beneficial to the technical and economic viability of chemical processing plants. Therefore, it was necessary to further optimise this on-purpose Bio-LPG process by investigating the effect of butanol concentration on the yields and composition of gas products. In previous sections, char formation remained low at less than 5 wt% of the n-butanol feed. However, due to the formation of substantial amounts of solid products during experiments in with high n-butanol concentrations, it became necessary to present the carbon balances in the reaction products (Table 2). As shown in the table, char formation increased with increasing loading of n-butanol due to oversaturation of the surface of the catalysts with reactant molecules. In addition, the inaccessibility of the active sites of the catalysts at high concentrations led to reduced conversion of butanol, hence increasing carbon contents in the liquid phase were observed. Therefore, while processing high concentrations of feedstock may be desirable, such conditions often lead to extensive char formation during thermochemical conversion of biomass via dehydration to form alkenes and stronger interactions between catalysts and unsaturated carbon atoms [24–26].
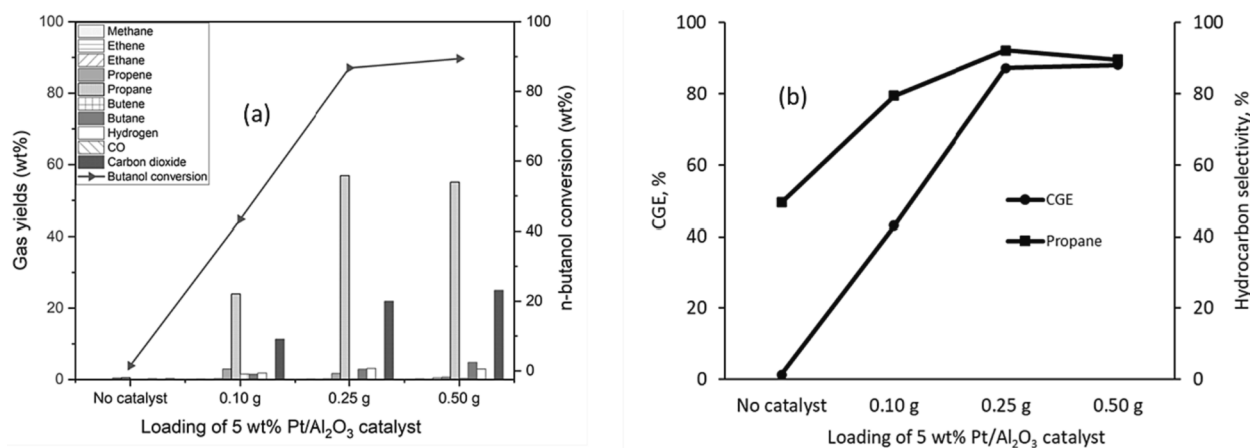

Fig. 3. Effect of 5 wt% Pt/Al_2O_3 catalyst loading on: (a) gas yields and conversion of 10 wt% aqueous butanol at 300 °C; (b) CGE and propane selectivity. (Reaction conditions: n-butanol/Pt metal molar ratios of 0, 1053:1, 421:1 and 211:1, respectively; initial pressure of N_2 of 5 bar).

Table 2
Carbon balance during catalytic hydrothermal conversion of n-butanol in relation to feedstock concentration at 300 °C, for 1 h reaction time.

Butanol concentration	Gas (wt%)	Liquid (wt %)	Solid (wt %)	wt% Balance
10 wt%	89.68 ± 2.08	8.94 ± 0.21	0.19 ± 0.01	98.81
15 wt%	76.52 ± 1.66	16.18 ± 0.40	4.38 ± 0.10	97.09
20 wt%	71.56 ± 1.78	19.01 ± 0.36	6.17 ± 0.12	96.52
30 wt%	60.92 ± 1.57	23.68 ± 0.18	9.57 ± 0.26	94.17

For this purpose, a series of experiments were carried out at 300 °C and a residence time of 1 h with increasing concentrations of n-butanol including 10 wt%, 15 wt%, 20 wt% and 30 wt% in water (corresponding to 2 g, 3 g, 4 g and 6 g of butanol) using a constant 5 wt% Pt/Al$_2$O$_3$ catalyst loading of 0.25 g. The results obtained are presented in Fig. 4, which showed that n-butanol conversion decreased from 86.7 % at a concentration of 10 wt% to 62.6 % when the concentration was increased to 30 wt%. In addition, there was a corresponding decrease in yield of propane from 56.88 % to 39.04 %, respectively.

The trends in both the carbon gasification efficiency and propane selectivity (Fig. 4b) show similar poor results with increasing n-butanol concentrations These results would be due to the over saturation of the catalyst active sites by the butanol at loadings > 10 wt% thereby causing reduction of catalytic activity. This observation agreed with the results obtained on effect of catalyst loading in Section 3.3 confirming that the n-butanol/Pt metal molar ratio of 421:1 gave the best results.

3.5. Possible reaction mechanisms for n-butanol conversion

A reaction scheme with various pathways based on the gases produced during the reaction of n-butanol in this present work is proposed and shown in Scheme 2. Clearly, the participation of water in Reaction Step 1 must be considered to explain the yields of hydrogen and CO$_2$ from possible direct deformylation of n-butanol or dehydrogenation of n-butanol to butanal followed by decarbonylation (Steps 5 and 6) [12].

The deformylation pathway (Step 1) would give propane and HCHO, and the latter would quickly react with water molecules to make one mole of CO$_2$ and 2 mol of H$_2$. Also, the dehydrogenation/decarbonylation pathway (Steps 5 and 6) would produce propane, H$_2$ and CO, with the CO further undergoing water–gas shift reaction to make one more mole of H$_2$ and one mole of CO$_2$. Therefore, these two pathways would essentially give the same products and can both be represented by

the same overall reaction Equation (6).

$$C_4H_9OH + H_2O \rightarrow C_3H_8 + CO_2 + 2H_2 \qquad (6)$$
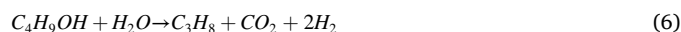
Further experimental tests were carried out to understand further details about Equation (6). Considering the low stability of HCHO (deformylation product) under hydrothermal/steam conditions, these tests were carried out dry (without adding water to the reactor). First, 2 g of n-butanol and 1 g of 5 wt% Pt/Al$_2$O$_3$ catalyst only were loaded into the reactor and heated to 300 °C. The reaction was stopped by withdrawing the reactor from the heater upon reaching 300 °C (zero minute) and cooled rapidly with the laboratory fan. In this test, n-butanol yielded around 27 wt% of gas products, which contained propane (10.2 wt%), butane (9.10 wt%), propene (1.26 wt%), methane (0.12 wt%), H$_2$ (0.28 wt%), CO$_2$ (3.63 wt%) and CO (2.31 mol%). The gas product from this test also gave a small unknown peak at 7.5 min (*Supplementary Information Figure SI1*). This unknown peak was confirmed to be formaldehyde by the analysis of the gas product obtained from the reaction of methanol with the 5 wt% Pt/Al$_2$O$_3$ at 300 °C for zero minute (*Supplementary Information Figure SI1*) [27].

Thereafter, the same reaction was repeated at 300 °C for 1 h reaction time and n-butanol conversion increased to 34.9 wt%, while the yields of propane and butane increased slightly to 12. 8 wt% and 10.3 wt%, respectively. However, the yields of other gas components changed dramatically. There were reductions in the yields of propene (0.45 wt%), H$_2$ (0.15 wt%) and CO (0.71 wt%), while significant increases in the yields of CO$_2$ (7.44 wt%) and methane (1.30 wt%) were observed. No peak was observed at 7.5 min after the one-hour reaction (*Supplementary Information Figure SI1*), which showed the quick conversion of HCHO. The variation in the yields of H$_2$ and CO during these reactions supported their formation from HCHO under both aqueous and non-aqueous conditions (reaction (*Supplementary Information Figure SI2*).

These results showed that the mechanisms for formation of propane and butane were equally dominant and may also explain the initial mechanisms under hydrothermal conditions. These could be explained as follows: in the absence of water, the deformylation (Step 1) combined with dehydrogenation of HCHO or combination of Step 5 and Step 6 in Scheme 2 yielded propane, CO and H$_2$. A second pathway involving the dehydration of n-butanol to butene must have occurred in parallel. The co-production of water from the n-butanol dehydration pathway could have promoted water–gas shift reaction of CO to make H$_2$ and CO$_2$. Therefore, in the initial stages of the n-butanol conversion (shown by the zero-minute non-aqueous test), the hydrogen produced was mainly used to hydrogenate butene to butane. However, with increased reaction time (1 h), more hydrogen was produced, and the catalyst may have promoted its use for methanation of CO to methane, while producing more water for the CO – H$_2$ cycle. Although, no butanal was found or
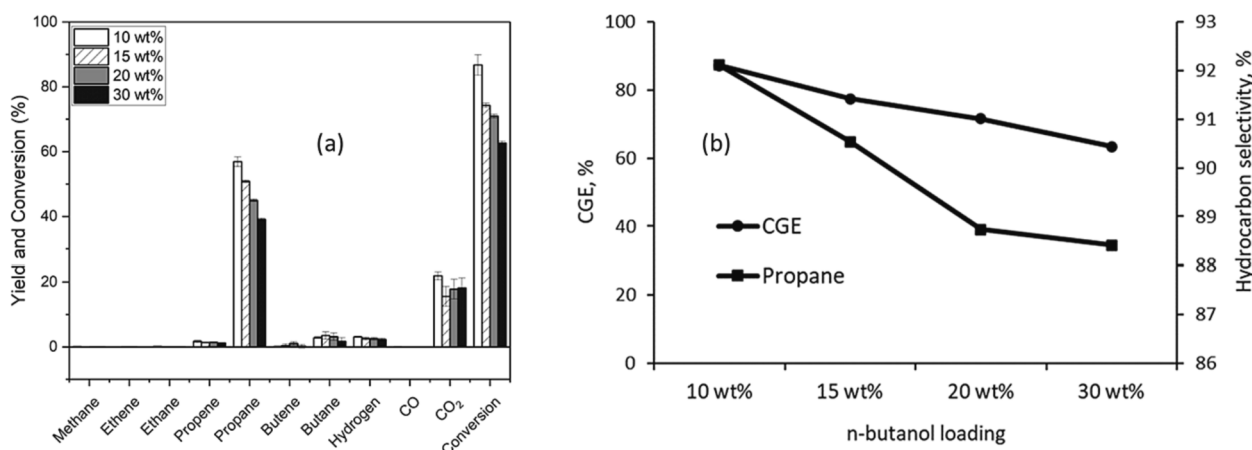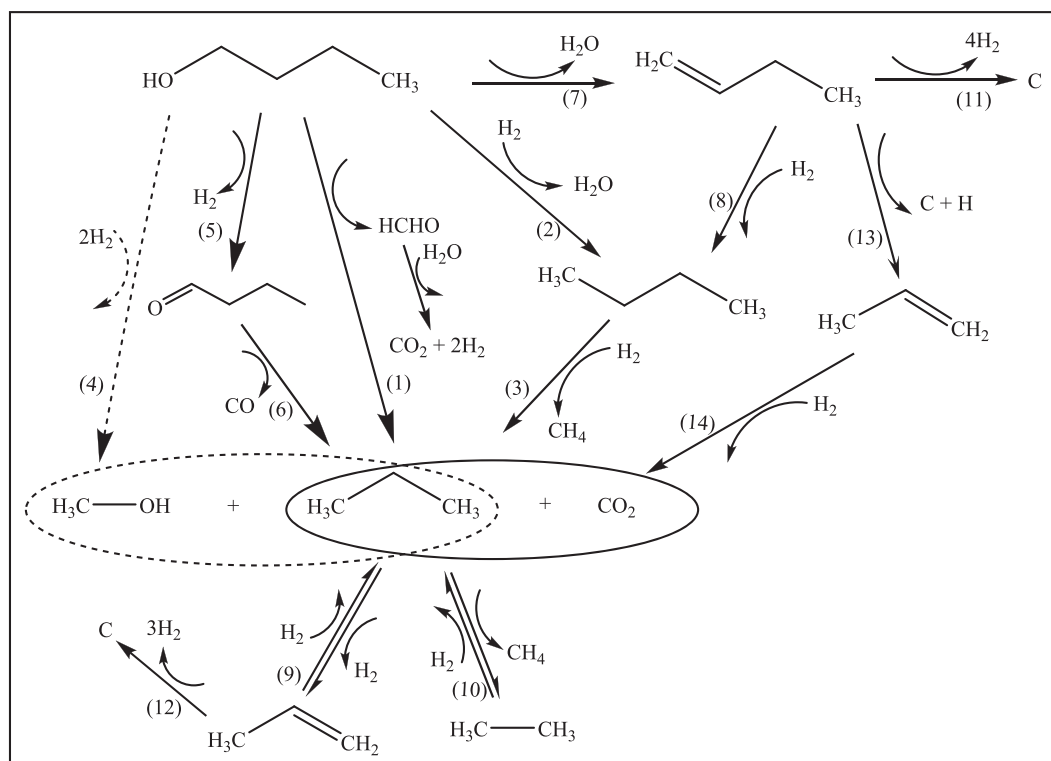

Fig. 4. Effect of n-butanol concentrations on gas yield and conversion of butanol at 300 °C. (Reaction conditions: n-butanol/Pt metal molar ratios of 421:1, 632:1, 842:1 and 1263:1, respectively; initial pressure of N$_2$ of 5 bar).

Scheme 2. Reaction pathway proposed from this study.

identified in the liquid phases obtained from these supplementary tests, its formation and rapid consumption under catalytic hydrothermal conditions of this present study was still a possibility.

In comparison, it could be inferred that the formation of propane from other pathways was promoted by the large presence of water during the hydrothermal experiments. For instance, Fig. 4a shows that much higher yields of propane corresponded to much lower yields of butane in hydrothermal media. Hence based on Equation (6), the theoretical yields of the gases from total feedstock conversion (total molecular masses of n-butanol and water = 92 g) would be 47.8 wt% of propane, 47.8 wt% of CO_2 and 4.4 wt% of hydrogen. Therefore, Reaction Step 1 would give a mass ratio of propane to CO_2 of 1:1, which was far below the mass ratios obtained from the experimental data (Fig. 5a). For instance, the analysis of the experimental results at different temperatures (Section 3.1) showed that the mass ratios of propane to CO_2 in the gaseous products were 2.57, 2.61 and 2.60 at 200 °C, 250 °C and 300

°C, respectively. This indicated that other propane-only forming reactions must have occurred, probably using the hydrogen produced from Reaction Step 1. Since the other gases were produced in trace amount, the yields of propane, butane, hydrogen and carbon dioxide were further considered in greater detail. The experimental results from the effect of reaction time (Section 3.2) showed that the final yield and hydrocarbon selectivity of propane in the gas must have resulted from multiple reaction pathways. Plausible reactions would be the C–O hydrogenolysis of butanol to butane according to Reaction Step 2, which is supported by literature [23]. Furthermore, the hydrogenation of butanol at the alpha C–C bond in Reaction step 4 could produce propane and methanol. According to Scheme 2, the formation of butane could follow two pathways: the direct C–O hydrogenolysis of n-butanol in Reaction Step 2 as well as the dehydration of butanol to butene in Reaction Step 5, followed by the hydrogenation of the butene to butane in Reaction Step 8. However, given that some butene remained in the gas products, it was
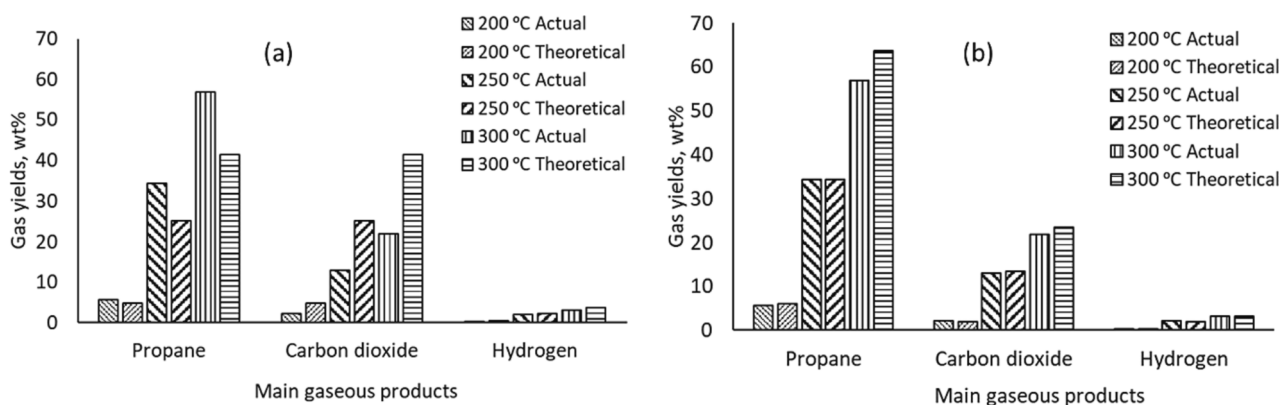

Fig. 5. Comparison of the theoretical and actual yields of the main gas components involved in the conversion of 10 wt% aqueous n-butanol in relation to temperature, based on: (a) stoichiometric reaction Equation (6); (b) idealised reaction Equation 7 (Reaction conditions: n-butanol/Pt metal molar ratio = 421:1); initial pressure of N_2, 5 bar; autogenic pressure of 7.7 bar, 18.7 bar and 26.6 bar at 200 °C, 250 °C and 300 °C, respectively).

likely that the butanol dehydration and hydrogenation pathways was favoured for butane formation [28].

Clearly, the final yields of butane were consistently up to 20 times lower than that of propane, indicating that the butene/butane pathways could produce propane. This could be through the possible hydrogenolysis of terminal C–C bonds in butane (Step 3) or butene via propene (Steps 13 and 14). Traces of methane and ethane were found at 300 °C, possibly due to the hydrogenolytic cracking of the C_3 and C_4 gases, particularly propane in Reaction Step 3 and 10.

Hence, based on detailed analysis of data obtained from the effects of temperature and reaction time, a proposed composite reaction, which could better explain the contributions of the reactions that gave the major products is proposed in (Equation 7).

$$3C_4H_9OH \rightarrow 3.2C_3H_8 + 0.8H_2 + 0.56C + 0.16C_4H_{10} + 1.2CO_2 + 0.6H_2O \quad (7)$$
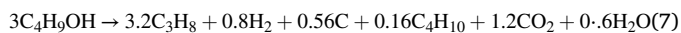
A comparison of the actual yields of propane, hydrogen and carbon dioxide with their predicted yields based on Equation 7 is presented in Fig. 5b. The results show better agreements for the experimental yields of the three gas products compared to the stoichiometric pathway represented by Equation (6).

3.6. Reusability and stability of the 5 wt% Pt/Al₂O₃ catalyst

The reusability and stability of the Pt/Al₂O₃ was investigated for the conversion of butanol to propane. Four cycles of experiments were performed under the same reaction condition (300 °C for 1 h) starting with fresh 0.25 g of Pt/Al₂O₃ and 2 g of butanol in water with and without calcination of the catalyst before each cycle. The calcination step was necessary to eliminate the possibility of loss of catalytic activity due to carbon deposited from butanol, and possibly to restore the active phase of the alumina support. Multiple reactions were performed at each cycle to ensure that 0.25 g of catalyst material was available for the sequential reactions. The results obtained are presented in Fig. 6.

On the one hand, for reactions with calcined catalyst the conversion of butanol for first, second, third and fourth use were 86.74 %, 84.06 %, 24.10 % and 7.18 %, respectively. Propane yields decreased by nearly 8 % when the catalyst was reused the second time after calculation. Subsequent repeated use of the recalcined catalyst gave dramatic reduction of propane yields to 14.35 % and 3.29 % during the third and fourth cycles, respectively (Fig. 6a). On the other hand, repeat reaction cycles performed without calcining the used catalysts gave much lower butanol conversion at the second use, reducing by 31.2 % compared to the fresh catalyst. Dramatic reduction in butanol conversion was also

observed at the third and fourth use, but these reductions where smaller compared to the calcined catalyst as shown in Fig. 6b.

For the uncalcined catalyst, the corresponding yields of propane were 56.88 %, 45.53 %, 23.21 % and 5.99 % over the four reaction cycles. The results obtained for both scenarios showed that the catalyst activity showed considerable stability at the second use, with comparable results with the fresh catalyst use. Beyond the second use, activity declined significantly. This result is in tune with that of Yadav and Vaidya [29], who found a decrease in catalytic activity of Pt/Al₂O₃ for the steam reforming of butanol to hydrogen after one hour, due to support structure collapse via alumina hydrolysis.

Pt/Al₂O₃ is a frequently used catalyst in hydrothermal process [30] and investigations on the alumina support show its likelihood to undergo changes in crystalline properties under high temperatures and extended reaction times [18,31]. This could explain the higher rate of decreasing catalytic activity was observed for reactions in this present study with the calcined catalyst compared to the uncalcined [30. 31]. However, to enable the C–C and C-O bond cleavage of butanol to produce high yields of propane in the hydrothermal process, the stability of catalyst active sites is vital. The results in Fig. 7a and 7b mirror the trend in the loss of catalytic activity during repeated use. Indeed, at the fourth repeat cycle, the CGE had dramatically reduced but were still slightly higher than the results from the non-catalytic test in Section 3.3, indicating some level of catalytic activity.

3.7. Characterization of fresh and spent catalysts

In view of these findings from reusability of the Pt/Al₂O₃ catalyst, further investigations on the catalyst stability were carried out to obtain insight into the catalyst activity and determine the possibility of the catalyst to undergo structural changes during the hydrothermal process that could result in its deactivation. For this purpose, SEM and X-ray diffraction (XRD) measurements were performed on fresh and spent catalysts.

The XRD patterns obtained are shown in Fig. 8. The analysis of the fresh catalyst showed $2\theta°$ peaks at $39° - 40°$ corresponding to combined Pt metal and Al₂O₃, with subsequent Al₂O₃ peaks at $46°$ and $67°$. After hydrothermal treatment, the recovered catalyst showed Pt peaks and additional peaks corresponding to boehmite (Pt/AlO(OH)) and graphitic carbon [18]. The Pt presence in both fresh and recovered catalyst after the first cycle confirmed that the Pt metal was probably stable and suffered little or no losses during this cycle. However, it is also clear from the XRD patterns that the first and second cycle had similar peaks
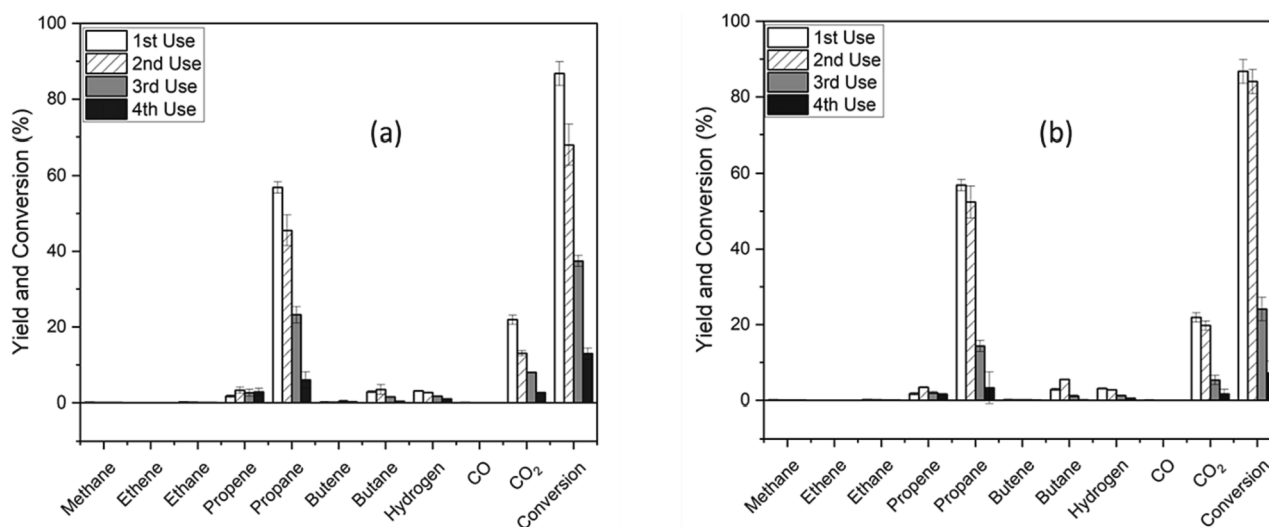

Fig. 6. Effect of reusing catalyst on gas yield and conversion of 10 wt% aqueous butanol solution at 300C: (a) without calcination; (b) after calcination. (Reaction conditions: n-butanol/Pt metal molar ratios of 421:1; initial pressure of N2 of 5 bar).
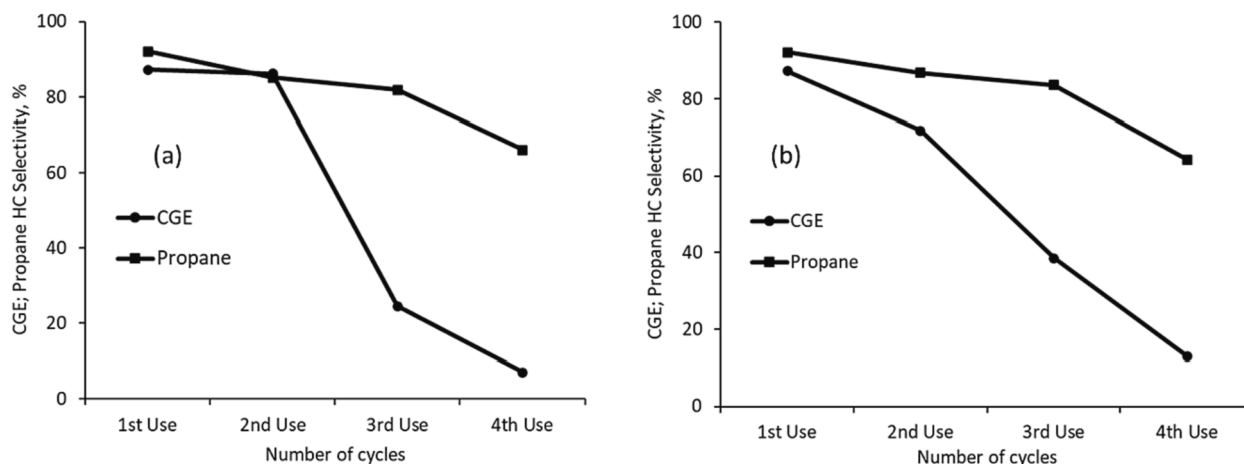
Fig. 7. Effect of reusing catalyst on CGE and propane hydrocarbon selectivity during the reaction of 10 wt% aqueous butanol solution at 300 °C: (a) without calcination; (b) after calcination. (Reaction conditions: n-butanol/Pt metal molar ratios of 421:1; initial pressure of N_2 of 5 bar).
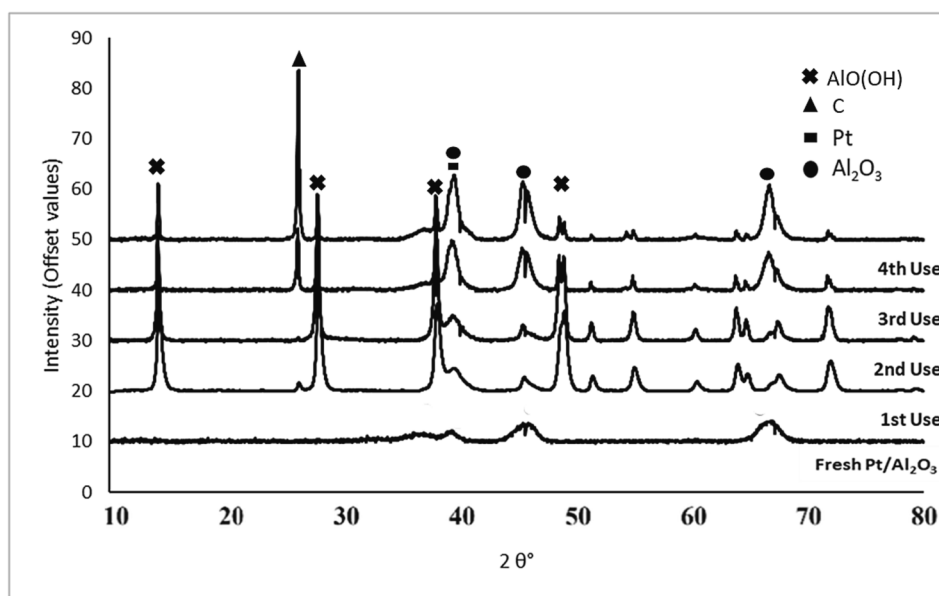

Fig. 8. XRD pattern of fresh and recovered 5 wt% Pt/Al_2O_3 over four reaction cycles, with clear changes in the structure and composition of the catalysts after repeated use.

(mostly boehmite formation) while the third and fourth cycle had similar peaks (boehmite and graphitic carbons).

Hence, the significant loss in catalytic activity observed over the 5 wt % Pt/Al_2O_3 catalyst after the second cycle in this study. This implied that the selective hydrothermal conversion of butanol to produce propane was largely suppressed by changes in the phases of the catalyst, which affected Pt metal dispersion and exposure for catalysis. Fig. 8 shows extensive presence of boehmite (AlO(OH)), with peaks at $2\Theta = 14°$ and $29°$ after the first experiment. Literature shows that alumina can transform to boehmite ($Al_2O_3 + H_2O \rightarrow 2AlO(OH)$) under hydrothermal conditions [32–34]. In addition, the weak signal of the Pt phase ($2\Theta = 39°$) in the fresh catalyst became enlarged with subsequent use, indicating the collapse of support structure, which affected metal dispersion and the catalytic activity. Extensive formation of char on the catalyst surface occurred during the third and fourth reaction cycles as shown by the sharp peaks of graphitic carbon at $2\Theta = 26.5°$. Hence, with the hydrolytic collapse of alumina support, the selectivity towards gas formation disappeared, which possibly promoted the dehydration of butanol for form alkenes. Hence, the lack of in situ generated hydrogen

gas, catalysed by the active sites of the catalyst, led for the conversion of alkenes to char. It appeared that the formation of boehmite could not be reversed even by calcination in this work. Indeed, it was observed that catalytic activity further reduced after calcination (Fig. 7), which could be because boehmite formation increased with time and temperature during the calcination procedure, which agreed with previous structural studies on Pt/Al_2O_3 [35,36].

The SEM images with resolution of x150 magnification are presented in Fig. 9. The SEM results revealed that the surface of the catalyst became rougher after the first use and led to complete distortion of the catalyst support at the end of the fourth cycle. These changes agree with those observed from the XRD analysis, confirming that the Pt/Al_2O_3 catalyst was unstable under the hydrothermal conditions used in this work. Hence, while Pt was effective for the selective conversion of butanol to propane, it would need a much more stable support to withstand the harsh hydrothermal conditions and maintain its catalyst activity for longer. Further efforts would be made in this area to enhance the commercial prospects of a butanol-to-propane process.
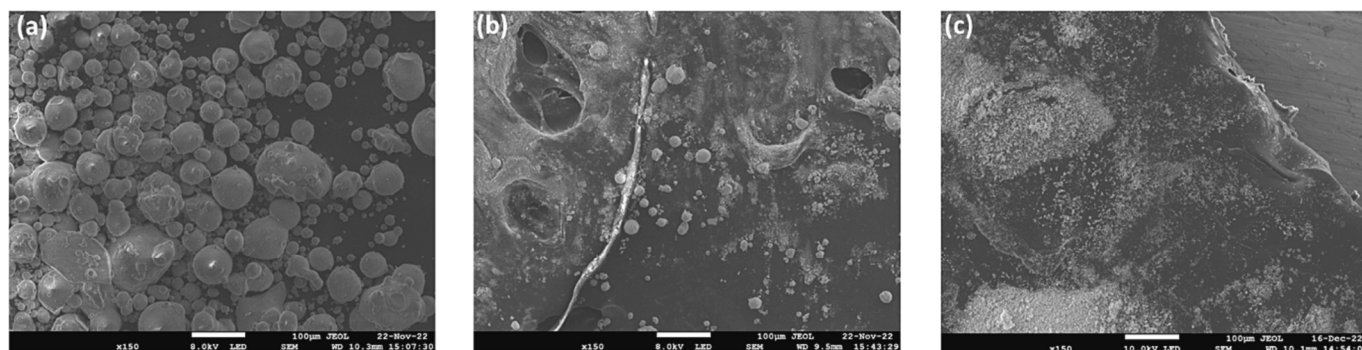
Fig. 9. SEM pattern of fresh and spent 5 wt% Pt/Al$_2$O$_3$: (a) fresh catalyst, (b) catalyst recovered from 1st cycle and (c) catalyst recovered from 4th cycle *(all images at x150 magnification, 8.0 KV and 100 μm resolution)*.

4. Conclusion

The conversion of n-butanol, which can be derived in high volumes from biomass to high yields of propane, presents a potentially viable pathway for on-purpose Bio-LPG production. In this present study, reactions have been carried out in a batch hydrothermal reactor with 5 wt % Pt/Al$_2$O$_3$ as catalyst. The investigations carried out included detailed parametric study which helped to propose the relevant reaction mechanisms. Results showed that the propane yield and butanol conversion increased with increase in temperature, residence time, amount of catalyst but decreased with increasing n-butanol concentrations. In all cases, the hydrocarbon selectivity toward propane was > 85 %, which supported the effectiveness of the catalyst to promote propane-forming reaction mechanisms. Deformylation (HCHO removal) of n-butanol or dehydrogenation of n-butanol to butanal followed by decarbonylation of butanal appeared to be the dominant mechanism for propane formation along with H$_2$ and CO$_2$. However, the unequal yields of propane and CO$_2$ indicated the occurrence of other propane-only forming reactions apart from deformylation. One plausible pathway was the dehydration of n-butanol to butene, followed by hydrogenation and C–C hydrogenolysis by the in-situ generated H$_2$ to make propane. Increased reaction severity in terms of increased temperature, increased reaction time and increased catalyst loading, led to the promotion of side reactions, such as cracking of higher alkane gases. The optimum propane yield and butanol conversion obtained were 56.88 % and 86.74 %, respectively, by reacting 10 wt% of butanol with 0.25 g of 5 wt% Pt/Al$_2$O$_3$ at 300 °C and 1 h residence time.

Reusing the catalyst showed stability for up to two reaction cycles after which significant loss of activity was observed. The catalyst deactivation was verified with SEM and XRD analyses and the loss in catalytic activity in this study was mainly due to the formation of boehmite from the hydrolysis gamma-alumina support during the hydrothermal process. Subsequent reuse of the catalyst at the third and fourth cycles showed coke formation on the catalyst surface, in addition to the hydrolysis of the alumina support. Future work would focus on finding more stable catalysts supports and reducing catalyst costs by replacing or reducing the loading of expensive metal catalysts. The high yields and selectivity of propane obtained from this work showed that n-butanol could become an excellent candidate feedstock for on-purpose large-scale production of the clean and low-carbon fuel gas.

CRediT authorship contribution statement

Onajite T. Abafe Diejomaoh: Investigation, Methodology, Data Curation, Validation, Visualization, Writing original draft. **Jude A. Onwudili:** Conceptualization, Funding acquisition, Methodology, Visualization, Supervision, Project administration, Writing original draft, Writing - review & editing. **Keith E. Simons:** Writing – review & editing, Supervision, Resources, Project administration. **Priscila Maziero:** Validation, Supervision, Resources, Project administration.

Declaration of competing interest

The authors declare the following financial interests/personal relationships which may be considered as potential competing interests: Jude Onwudili reports financial support was provided by Biotechnology and Biological Sciences Research Council. Jude Onwudili reports financial support was provided by Calor Gas Ltd. This work was co-funded by Calor Gas (UK) Limited, which is a subsidiary of SHV Energy, The Netherlands. Keith Simons and Priscila Maziero, co-authors of the paper, work for SHV Energy and Supergasbras (a subsidiary of SHV Energy), respectively. Both co-authors were involved in design of study and the decision to publish the results.

Data availability

Data will be made available on request.

References

[1] Johnson E. Process Technologies and Projects for BioLPG. Energies 2019:12. https://doi.org/10.3390/en12020250.

[2] Net Zero – The UK's contribution to stopping global warming – Report by The Committee on Climate Change. 2019. https://www.theccc.org.uk/publication/net-zero-the-uks-contribution-to-stopping-global-warming/. [Accessed 24 November 2023].

[3] Vispute TP, Huber GW. Production of hydrogen, alkanes and polyols by aqueous phase processing of wood-derived pyrolysis oils. Green Chem 2009;11(9):1433–45. https://doi.org/10.1039/B912522C.

[4] Rosillo-Calle F. A review of biomass energy – shortcomings and concerns. J Chem Technol Biotechnol 2016;91(7):1933–45. https://doi.org/10.1002/jctb.4918.

[5] Huber GW, Dumesic JA. An overview of aqueous-phase catalytic processes for production of hydrogen and alkanes in a biorefinery. Catal Today 2006;111(1): 119–32. https://doi.org/10.1016/j.cattod.2005.10.010.

[6] Schipper ELF, Boyd E. UNFCCC COP 11 and COP/MOP 1: At last, some hope? J Environ Dev 2006;15(1):75–90. https://doi.org/10.1177/1070496506286447.

[7] Hopwood L, Mitchell E, Sourmelis S. Biopropane: Feedstocks, Feasibility and our Future Pathway.Reports for the UK. https://www.liquidgasuk.org/uploads/DOC5DA5B52BBA49F.pdf; 2019. [Accessed 23 November 2023].

[8] UK LG. A Practical Approach - analysis of off-grid heat decarbonisation pathways; https://www.liquidgasuk.org/uploads/DOC5DA5B347CF3A7.pdf ;2019. [Accessed 23 November 2023].

[9] Johnson E. New biofuel debut: biopropane. Biofuels Bioprod Biorefin 2015;9(6): 627–9. https://doi.org/10.1002/bbb.1615.

[10] Johnson E. A carbon footprint of HVO biopropane. Biofuels Bioprod Biorefin 2017; 11(5):887–96. https://doi.org/10.1002/bbb.1796.

[11] Razaq I, Simons K, Onwudili J. Parametric study of Pt/C-catalysed hydrothermal decarboxylation of butyric acid as a potential route for biopropane production. Energies 2021;14:3316. https://doi.org/10.3390/en14113316.

[12] Roy B, Sullivan H, Leclerc CA. Aqueous-phase reforming of n-BuOH over Ni/Al_2O_3 and $Ni/CeO2$ catalysts. J Power Sources 2011;196(24):10652–7. https://doi.org/10.1016/j.jpowsour.2011.08.093.

[13] Verduyckt J, De Vos DE. Highly selective one-step dehydration, decarboxylation and hydrogenation of citric acid to methylsuccinic acid. Chem Sci 2017;8(4):2616–20. https://doi.org/10.1039/C6SC04541C.

[14] Mazziotta A, Madsen R. Ruthenium-catalyzed dehydrogenative decarbonylation of primary alcohols. Eur J Org Chem 2017;2017(36):5417–20. https://doi.org/10.1002/ejoc.201701173.

[15] Alves C, Onwudili J. Screening of nickel and platinum catalysts for glycerol conversion to gas products in hydrothermal media. Energies 2022;15:7571. https://doi.org/10.3390/en15207571.

[16] Jiang J, Li T, Huang K, Sun G, Zheng J, Chen J, et al. Efficient preparation of bio-based n-butane directly from levulinic acid over Pt/C. Ind Eng Chem Res 2020;59(13):5736–44. https://doi.org/10.1021/acs.iecr.0c00255.

[17] Zhang Y, Chen J, Yang Y, Jiao R. Breeding high-ration butanol strains of Clostridium acetobutylicum and application to industrial production. Industrial Microbiology (in Chinese) 1996;26:1–6.

[18] Onwudili JA, Scaldaferri CA. Catalytic upgrading of intermediate pyrolysis bio-oil to hydrocarbon-rich liquid biofuel via a novel two-stage solvent-assisted process. Fuel 2023;352:129015. https://doi.org/10.1016/j.fuel.2023.129015.

[19] Onwudili JA, Razaq I, Simons KE. Optimisation of propane production from hydrothermal decarboxylation of butyric acid using Pt/C catalyst: influence of gaseous reaction atmospheres. Energies 2021. https://doi.org/10.3390/en15010268.

[20] Borges ACP, Onwudili JA, Andrade HMC, Alves CT, Ingram A, Vieira de Melo SAB, et al. Catalytic supercritical water gasification of eucalyptus wood chips in a batch reactor. Fuel 2019;255:115804. https://doi.org/10.1016/j.fuel.2019.115804.

[21] Shi Y, Weller AS, Blacker AJ, Dyer PW. Conversion of butanol to propene in flow: A triple dehydration, isomerisation and metathesis cascade. Catal Comm 2022;164:106421. https://doi.org/10.1016/j.catcom.2022.106421.

[22] Palla VCS, Shee D, Maity SK, Dinda S. One-step conversion of n-butanol to aromatics-free gasoline over the HZSM-5 catalyst: effect of pressure, catalyst deactivation, and fuel properties as a gasoline. ACS Omega 2023;8(46):43739–50. https://doi.org/10.1021/acsomega.3c05590.

[23] Gürbüz EI, Hibbitts DD, Iglesia E. Kinetic and mechanistic assessment of alkanol/alkanal decarbonylation and deoxygenation pathways on metal catalysts. J Am Chem Soc 2015;137(37):11984–95. https://doi.org/10.1021/jacs.5b05361.

[24] Minowa T, Zhen F, Ogi T. Cellulose decomposition in hot-compressed water with alkali or nickel catalyst. J Supercritical Fluids 1998;13(1–3):253–9. https://doi.org/10.1016/S0896-8446(98)00059-X.

[25] Williams PT, Onwudili J. Subcritical and supercritical water gasification of cellulose, starch, glucose, and biomass waste. Energy Fuels 2006;20:1259–65. https://doi.org/10.1021/ef0503055.

[26] Ortiz FG, Campanario F, Ollero P. Supercritical water reforming of model compounds of bio-oil aqueous phase: acetic acid, acetol, butanol and glucose. Chem Eng J 2016;298:243–58. https://doi.org/10.1016/j.cej.2016.04.002.

[27] Deitermann M, Huang Z, Lechler S, Merko M, Muhler M. Non-classical conversion of methanol to formaldehyde. Chem Ing Tech 2022;94:1573–90. https://doi.org/10.1002/cite.202200083.

[28] Harju H, Lehtonen J, Lefferts L. Steam reforming of n-butanol over Rh/ZrO_2 catalyst: role of 1-butene and butyraldehyde. Appl Catal B: Environ 2016;182:33–46. https://doi.org/10.1016/j.apcatb.2015.09.009.

[29] Abhimanyu K. Yadav, Prakash D. Vaidya. A study on the efficacy of noble metal catalysts for butanol steam reforming. Int J Hydrogen Energy 2019;44(7):25575–88. https://doi.org/10.1016/j.ijhydene.2019.07.191.

[30] Fisk CA, Morgan T, Ji Y, Crocker M, Crofcheck C, Lewis SA. Bio-oil upgrading over platinum catalysts using in situ generated hydrogen. Appl Catal A 2009;358(2):150–6. https://doi.org/10.1016/j.apcata.2009.02.006.

[31] Fasolini A, Cespi D, Tabanelli T, Cucciniello R, Cavani F. Hydrogen from renewables: a case study of glycerol reforming. Catalysts 2019;9(9):722. https://doi.org/10.3390/catal9090722.

[32] Shkolnikov EI, Shaitura NS, Vlaskin MS. Structural properties of boehmite produced by hydrothermal oxidation of aluminum. J Supercrit Fluids 2013;73:10–7. https://doi.org/10.1016/j.supflu.2012.10.011.

[33] Panda PK, Jaleel VA, Usha Devi S. Hydrothermal synthesis of boehmite and α-alumina from Bayer's alumina trihydrate. J Mater Sci 2006;41:8386–9. https://doi.org/10.1007/s10853-006-0771-7.

[34] Mukhamed'yarova AN, Egorova SR, Nosova, OV, Lamberov, AA. Influence of hydrothermal conditions on the phase transformations of amorphous alumina. Mendeleev Commun 2021;31(3):385–7. https://doi.org/10.1016/j.mencom.2021.04.034.

[35] Koichumanova K, Vikla AKK, de Vlieger DJM, Seshan K, Mojet BL, Lefferts L. Towards stable catalysts for aqueous phase conversion of ethylene glycol for renewable hydrogen. ChemSusChem 2013;69:1717–23. https://doi.org/10.1002/cssc.201300445.

[36] Mao Q, Guo Y, Liu X, Shakouri M, Hu Y, Wang Y. Identifying the realistic catalyst for aqueous phase reforming of methanol over Pt supported by lanthanum nickel perovskite catalyst. Appl Catal B: Environ 2022;313:121435. https://doi.org/10.1016/j.apcatb.2022.121435.